

Assessment and mapping of the shallow geothermal potential in the province of Cuneo (Piedmont, NW Italy)

*Original*

Assessment and mapping of the shallow geothermal potential in the province of Cuneo (Piedmont, NW Italy) / Casasso, Alessandro; Sethi, Rajandrea. - In: RENEWABLE ENERGY. - ISSN 0960-1481. - ELETTRONICO. - 102:part B(2017), pp. 306-315. [10.1016/j.renene.2016.10.045]

*Availability:*

This version is available at: 11583/2658035 since: 2016-11-29T09:58:59Z

*Publisher:*

Elsevier

*Published*

DOI:10.1016/j.renene.2016.10.045

*Terms of use:*

This article is made available under terms and conditions as specified in the corresponding bibliographic description in the repository

*Publisher copyright*

Elsevier postprint/Author's Accepted Manuscript

© 2017. This manuscript version is made available under the CC-BY-NC-ND 4.0 license  
<http://creativecommons.org/licenses/by-nc-nd/4.0/>. The final authenticated version is available online at:  
<http://dx.doi.org/10.1016/j.renene.2016.10.045>

(Article begins on next page)

# 1 Assessment and mapping of the shallow 2 geothermal potential in the province of 3 Cuneo (Piedmont, NW Italy)

---

4 Authors: Alessandro Casasso, Rajandrea Sethi \*

5 \* corresponding author

6 DIATI – Politecnico di Torino, corso Duca degli Abruzzi 24, 10129 Torino (Italy)

7 Telephone number: +39 0110907735

8 [alessandro.casasso@polito.it](mailto:alessandro.casasso@polito.it) , [rajandrea.sethi@polito.it](mailto:rajandrea.sethi@polito.it)

9 Post-print of the article published at:

10 <http://www.sciencedirect.com/science/article/pii/S0960148116309107>

## 11 Abstract

12 Ground Source Heat Pump (GSHP) is a low carbon heating and cooling technology which can make an  
13 important contribution for reaching the ambitious CO<sub>2</sub> reduction targets set by the European Union. The  
14 economic and technical suitability of this technology strongly depends on the thermal and hydrogeological  
15 properties of the ground at the installation site, which need to be assessed in detail. A common indicator  
16 adopted to define such suitability is the geothermal potential, i.e. the thermal power that can be  
17 exchanged with the ground through a GSHP with a certain setup. In this paper, we present the assessment  
18 and mapping of the shallow geothermal potential in the province of Cuneo, a 6,900 km<sup>2</sup> wide county in NW  
19 Italy. Geological, hydrogeological and climatic information are collected and processed to estimate the  
20 relevant ground properties. The shallow geothermal potential is then estimated with different methods for  
21 closed-loop installations (Borehole Heat Exchangers, BHEs) and open-loop installations (Ground Water Heat  
22 Pumps, GWHPs) systems in order to identify the most suitable areas for different technologies. The maps of  
23 the geothermal potential are an important planning tool for the installation of GSHPs and for the growth of  
24 this renewable energy source.

25 **Keywords:** geothermal potential; Ground Source Heat Pump; Borehole Heat Exchanger; Ground Water  
26 Heat Pump; Cuneo; heat pump

## 27 1 Introduction

28 The European Union recently set three ambitious objectives for its energy policies: by the year 2020, the  
29 total energy consumption and the Greenhouse Gas emission have to be cut by 20%, and 20% of the total

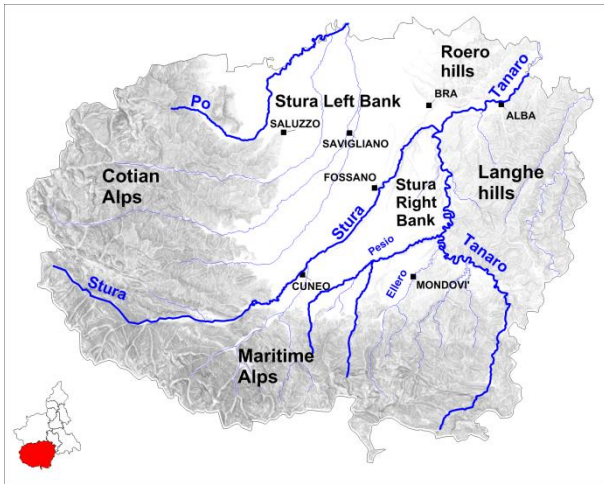
30 energy consumption should be covered by Renewable Energy Sources (RES) [1]. Italy has already achieved  
31 its national target in 2014, with 38.6% of the electricity and 18% of the heat production provided by RES [2],  
32 one of the best performances among EU Member States [1]. To achieve further improvements in alignment  
33 with Roadmap 2050 [3], efforts should now concentrate on heat production, for which the most adopted  
34 RES are ligneous biomass (68.9%) and heat pumps (25.8%) [2]. A further expansion of biomass heating is  
35 hardly sustainable, due to its impact on air quality [4, 5]. On the other hand, heat pumps have zero  
36 emissions on site and reduce GHG emissions up to 90% compared to fossil fuel burners, depending on the  
37 energy mix adopted for the production of electricity [6, 7]. In Italy, about 60% of the total production of  
38 electricity is covered by fossil fuels, with an emission factor of 326.8 g CO<sub>2</sub>/kWh [8]; the consequent  
39 reduction of CO<sub>2</sub> production, according to Saner et al. [7], is of about 50% compared to a methane boiler.  
40 Heat pumps are divided into two main categories: Air Source (ASHP) and Ground Source (GSHP). The main  
41 advantage of GSHPs compared to ASHPs is the higher COP, thanks to the lower temperature difference  
42 between the heat source (ground or groundwater) and sink (heating/cooling terminals) [9]. GSHPs have  
43 proved to be a cost-effective solution for a wide range of buildings, despite the additional expense for the  
44 installation of the ground heat exchangers .  
45 GSHPs in Italy still account for only 0.1% of the total thermal energy production [2]. However, a  
46 continuously increasing trend has been observed in recent years (+13% in 2013), and a strong rise is  
47 expected for the next 10-15 years [10, 11]. The high cost of installation is widely acknowledged as a limiting  
48 factor for the increase of heat pump installations and, particularly, for geothermal heat pumps. In Italy,  
49 another major barrier is the high cost of electricity for domestic supply, compared to the relatively low cost  
50 of methane [12]. As a consequence, compared to other countries, a lower saving margin is achieved for  
51 heat pumps against fossil-fuelled boilers. The problem of the higher cost of installation has been addressed  
52 introducing a strong tax refund (65%) on energy retrofit works of existing buildings, among which GSHPs  
53 are included [13].  
54 The lack of homogeneous and targeted regulation is another barrier for the growth of shallow geothermal  
55 energy in Italy [14]. This absence of regulation has been partially filled with voluntary schemes and  
56 standardization [15], such as the recent UNI standards for GSHPs [16-18].  
57 A final problem is that the technology and the potential of shallow geothermal energy are still little known  
58 in most EU countries. A number of EU-funded projects have been conducted in recent years to disseminate  
59 knowledge on GSHPs with training events, workshops, and case studies [19-21]. These projects raised the  
60 different stakeholders' awareness of the potential applications of shallow geothermal energy.  
61 However, the suitability of different territories for GSHPs needs to be studied on the small scale, since it  
62 depends on site-specific parameters and on the technology adopted [22-24]. A commonly adopted  
63 indicator is geothermal potential, which is defined in different ways, but can generally be identified as the

64 capacity of the ground/aquifer to provide heating and/or cooling [25-31]. Some projects have already been  
65 conducted in Italy to assess shallow geothermal potential. Busoni et al. [26] assessed and mapped the  
66 suitability for the installation of BHEs of the province of Treviso (Veneto, NE Italy). Their work took into  
67 account ground thermal conductivity, geothermal gradient and groundwater velocity. The VIGOR project  
68 [28, 29] addressed both shallow and deep geothermal energy potentials of four regions in Southern Italy  
69 (Campania, Apulia, Calabria and Sicily). In situ measurements of the thermal conductivity of rocks [28] were  
70 conducted over the mapped territory, and the potential for GSHPs was mapped for both heating and  
71 cooling purposes [29]. Gemelli et al. (2011, [30]) assessed the shallow geothermal potential of the Marche  
72 region (Central Italy), evaluating the required BHE length to cover a standard thermal load. Fewer studies  
73 have been performed for open loop Ground Water Heat Pumps (GWHPs), such as the works of Arola et al.  
74 in Finland [25]. Lo Russo and Civita provide an overview of the hydrodynamic properties of shallow  
75 unconfined aquifers in Piedmont (NW Italy) [31].

76 The aforementioned studies provide a methodological basis for the work presented in this paper. Here, the  
77 shallow geothermal potential in the province of Cuneo (Piedmont, NW Italy) is assessed and mapped. The  
78 geological and hydrogeological setting of this territory is studied, and a conceptual model is provided to  
79 correlate this setting with ground thermal parameters. These are the input for the estimation of the closed-  
80 loop geothermal potential with model G.POT [27]. The geothermal potential for open-loop systems was  
81 evaluated by estimating the maximum extractable and injectable flow rates of the shallow aquifers of the  
82 Cuneo plain, based on a dataset of well tests results. Conclusions are drawn on the suitability of different  
83 areas of the province of Cuneo for closed and open loop geothermal heat pumps.

## 84 **2 The territory surveyed**

85 The province of Cuneo is a 6,900 km<sup>2</sup> wide area located in the south-western edge of Piedmont. It can be  
86 subdivided into three main parts (Fig. 1): the Alpine valleys (Cotian and Maritime Alps) on the western and  
87 southern edges, covering about 51% of the total surface, the plain in the centre of the Province (22%) and  
88 the hills of Langhe and Roero in the East part (27%).



89

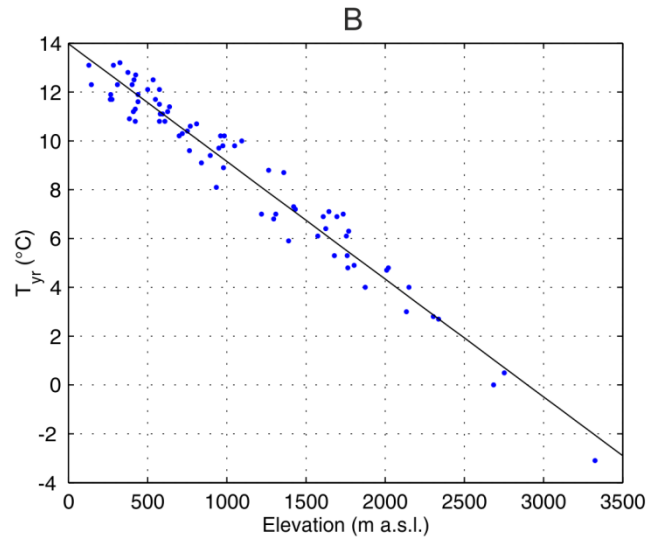
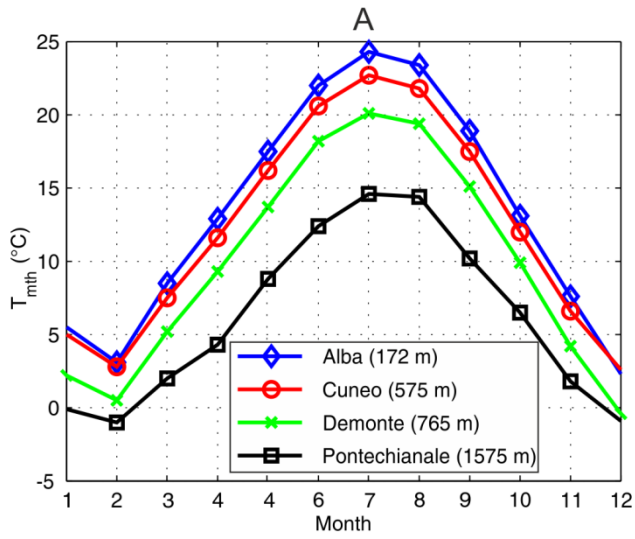
90 **Fig. 1 – Map of the province of Cuneo. Scale: 1:1,500,000.**

91 The total population is 592,060 inhabitants, of which 35% live in the county seat Cuneo (56,113 inhabitants)  
 92 and 6 other main towns in the plain (Alba, Bra, Fossano, Mondovì, Savigliano and Saluzzo) of 15,000 to  
 93 30,000 inhabitants. The rest of the population mostly lives in rural villages on the plain, while a small part  
 94 lives in the mountains and the hills.

95 In this chapter, the province of Cuneo is described from the climatic, geologic and hydrogeological points of  
 96 view, and data is provided for the assessment of the shallow geothermal potential.

97 **2.1 Climate**

98 Cuneo is characterized by a continental climate with a cold winter and a mild summer, as reported in Fig.  
 99 2A. Although the distance from the sea is quite short (30÷100 km), a weak influence of the Mediterranean  
 100 sea is observed, due to the isolating effect of the Alpine chain. The total rainfall varies widely, from  
 101 700÷900 mm/y in the hills of Langhe and Roero to 900÷1200 mm/y in the plain and in the mountains [32].  
 102 The annual mean air temperature is strongly correlated with the ground elevation, as shown in Fig. 2B,  
 103 ranging from -3.1°C to +13.2°C [33]. The climate of Cuneo and its province is therefore one of the coldest in  
 104 Italy, thus influencing the distribution of the heating degree-days (Italian DPR 412/1993 [34]). 66% of the  
 105 population lives in climate zone E (2400÷3000 heating DD) and 34% lives in climate zone F (>3000 DD). As a  
 106 consequence, the expense for house heating is one of the highest in Italy, while almost 90% of homes have  
 107 no chilling plant [35].



108

109

110

Fig. 2 – Climate of the province of Cuneo: (A) monthly mean temperatures in different locations; (B) correlation between elevation and mean annual air temperature.

111

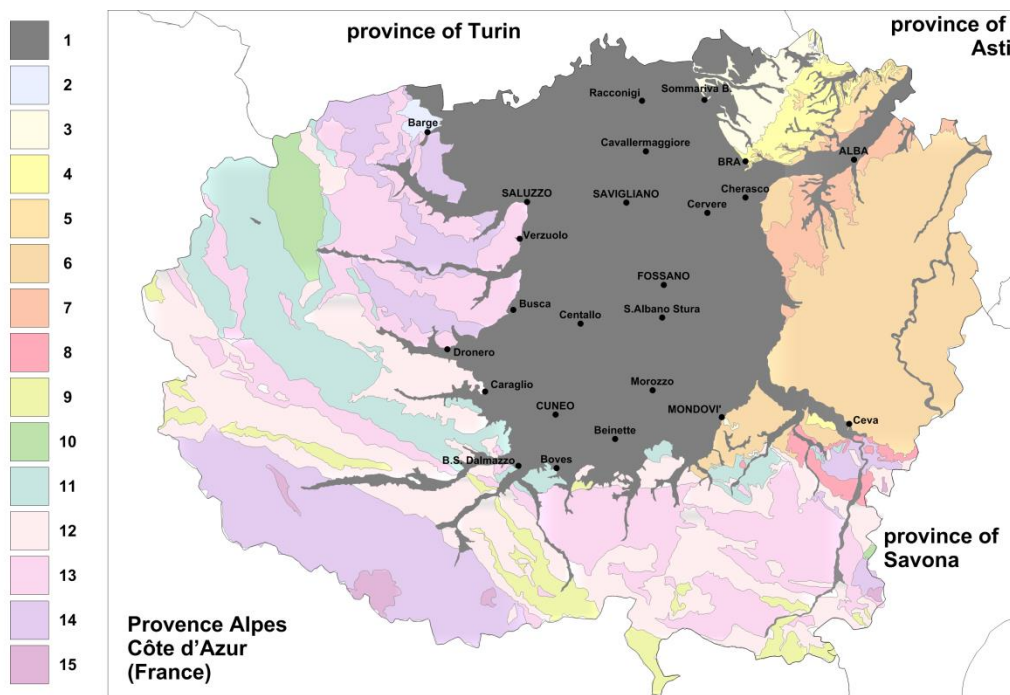
112

113 **2.2 Geology**

114 The mountainous portion of the territory surveyed is located on the boundary between the Helvetic and  
115 the Penninic domains of the Alps [36] and, according to the geological map of Piedmont [37] reported in  
116 Fig. 3, it is mainly composed of gneiss, and, to a lesser extent, limestone, calceschysts, serpentinites,  
117 sedimentary rocks (conglomerates, sandstone, gypsum, consolidated clays) and granite.

118 The plain is composed of locally cemented sand and gravel sediments deposited in the Holocene (12000  
119 years BP), with small loamy and clayey lenses. This alluvial cover lies on the Tertiary Piedmont Basin,  
120 composed of marine sediments settled during the Pliocene and the Villafranchian (5÷1 Ma BP) [31, 38].

121 The East part of the province of Cuneo is occupied by the hills of the Langhe, on the right bank of the  
122 Tanaro river, and of Roero, on the left bank. These hills were formed by the local uplifting of the Tertiary  
123 Piedmont Basin (Langhian, 16÷13 Ma BP) [39] and the excavated by the tributaries of the Tanaro river after  
124 the capture of this watercourse, occurred in the Riss-Wurm interglacial period (250,000 years BP). Langhe  
125 hills are mainly composed of Miocene marls and sandstones (23÷5 Ma BP), while Roero hills are composed  
126 of fine sands and clays deposited during the Pliocene (5÷2.5 Ma BP).



127 LEGEND OF LITHOLOGIES: 1) Alluvial sediments (Quaternary); 2) Moraines (Pleistocene); 3) Clays (Villafranchian); 4) Fine sands (Astian);  
5) Clays and clayey marls (upper Miocene - medium Pliocene); 6) Marls (medium Miocene); 7) Marls and siltstones (upper Oligocene-medium Miocene);  
8) Sandstone (Oligocene); 9) Alternated clayey layers (Cretaceous-Eocene); 10) Serpentinites of the Piedmontese zone (Jurassic-Cretaceous);  
11) Calceschysts of the Piedmontese zone (Jurassic-Cretaceous); 12) Limestones and dolomies (Mesozoic);  
13) Fine-grained gneiss of the Dora-Maira Massif (Permian); 14) Coarse-grained gneiss of Monte Rosa and Val d'Ossola (Permian); 15) Granites (Permian)

128 **Fig. 3 – Geological map of the province of Cuneo (adapted from ARPA Piemonte [40]). Scale: 1:1,000,000.**

129

## 130 2.3 Hydrogeology

131 The capture of Tanaro affected not only the morphology of a large part of the territory surveyed, but also  
132 the underground water circulation. Indeed, the deepening of the river bed of Tanaro's tributaries  
133 transformed them into hydraulic divides of the alluvial unconfined aquifer, which is composed of three  
134 main portions [32] (Fig. 4): the *Left Stura Bank* and the *Right Stura Bank*, separated by the river Stura, and  
135 the *Tanaro Valley* along the river.

136 The *Left Stura Bank* is a large aquifer (1117 km<sup>2</sup>) in the Western sector of the plain. The subsurface flow is  
137 directed from SW to NNE (Fig. 4A,) and the hydraulic gradient gradually diminishes from 10‰ on the West  
138 and South edges to 2‰ in the North part of the plain. The transmissivity is very high (up to 0.1 m<sup>2</sup>s<sup>-1</sup>) in the  
139 centre and diminishes on the eastern edge, with a concurrent reduction of the saturated thickness (Fig. 4B)  
140 of the aquifer [31]. The depth to water table (Fig. 4A) is below 10 m in the central part of the plain, while  
141 higher values close to the East and West boundaries, up to 70 m in the South-Western portion.

142 The *Right Stura Bank* aquifer (523.5 km<sup>2</sup>) is divided into a number of sub-sectors due to the influence of the  
143 creeks Pesio, Ellero and other smaller water courses [38]. On a narrow strip along the Stura river, the  
144 average transmissivity is quite high ( $5 \cdot 10^{-3} \div 5 \cdot 10^{-2}$  m<sup>2</sup>s<sup>-1</sup>) [31], while in the rest of this area is much lower  
145 ( $< 10^{-3}$  m<sup>2</sup>s<sup>-1</sup>). The saturated thickness is about 50 m in the SW portion along the Stura and it decreases to  
146 5 ÷ 10 m elsewhere, with a sharp transition; a similar trend is observed for the depth to water table.

147 The narrow aquifer of *Tanaro Valley* is scarcely productive [32] and, together with the other small aquifers  
148 located in the valleys and on the Langhe and Roero hills, it is not considered in the analysis of the open-loop  
149 geothermal potential.

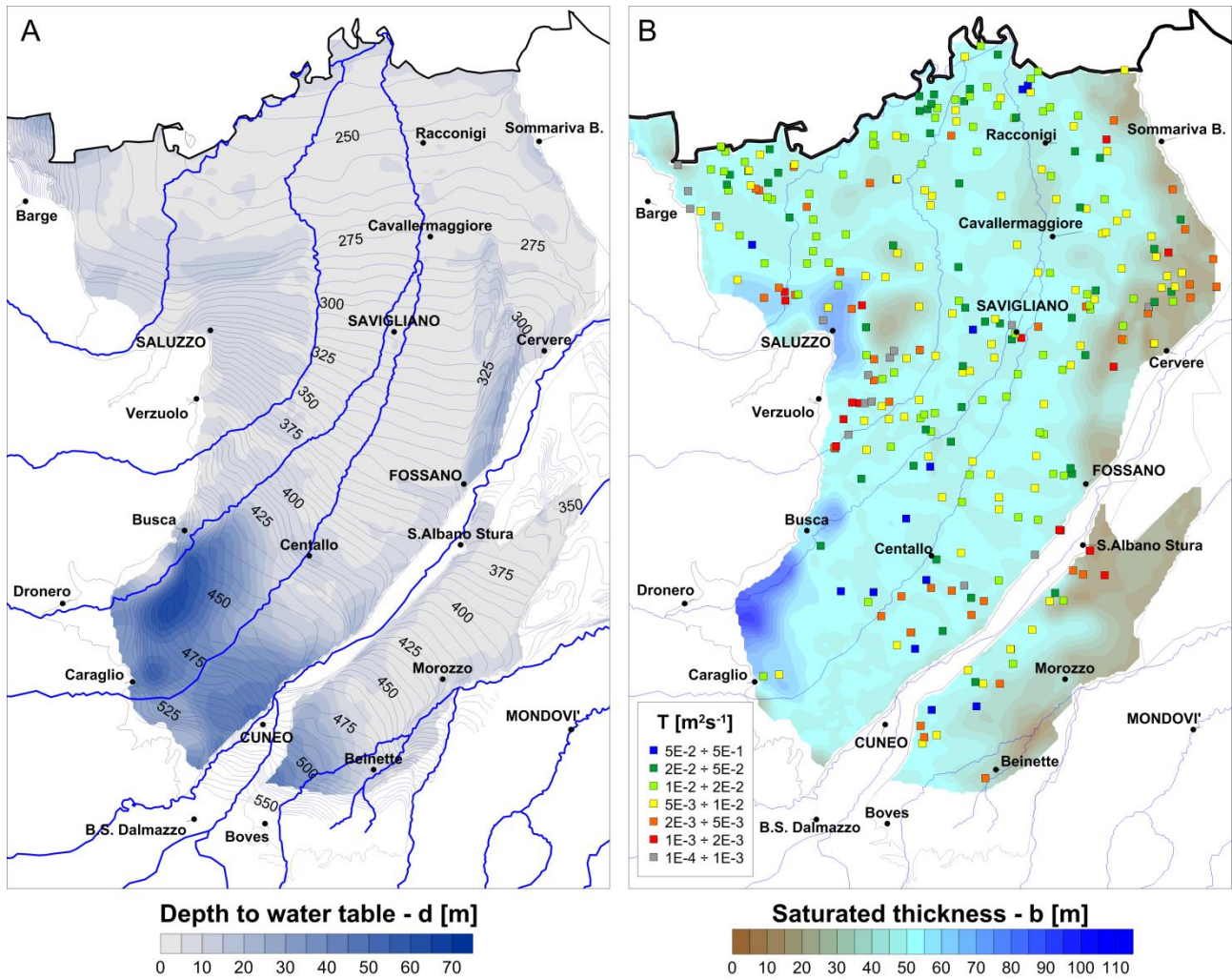
## 150 3 Shallow geothermal potential

151 The spatial distributions of thermal and hydrogeological parameters, reported and described in the  
152 previous chapter, were used to assess the techno-economic feasibility of shallow geothermal systems in  
153 different parts of the province of Cuneo. The geothermal potential has different definitions depending on  
154 the technology adopted, i.e. closed-loop (BHE) or open-loop (GWHP).

155 For closed-loop systems it is defined, according to G.POT [27], as the yearly average thermal load that can  
156 be exchanged with the ground by a BHE with a length  $L$ , coping with a minimum/maximum temperature  
157 threshold of the heat carrier fluid. A limit is therefore imposed to the thermal alteration of the heat carrier  
158 fluid, which mostly depends on the thermal parameters of the ground and, to a lesser extent, on the  
159 characteristics of the BHE itself [22].

160 On the other hand, heat transport in GWHPs mostly depends on the hydrodynamic parameters of the  
161 aquifer, while thermal conductivity has a minor impact on the heat diffusion into the aquifer [41]. The  
162 efficiency of these systems can be impaired by thermal recycling, which should be considered in the design

163 phase using analytical or numerical models [24, 42]. Another important aspect of the design of GWHPs is  
164 the propagation of thermal plumes downstream the injection well, with a negative impact on drinking  
165 water wells or other geothermal installations. These issues are more likely in large cities with a high density  
166 of GWHPs [43, 44], rather than in a scarcely populated territory such as the province of Cuneo. Both the  
167 issues of thermal recycling and thermal plume interference should be evaluated with consideration to  
168 specific plants and setups, and hence a large-scale assessment is not feasible. On the other hand, the  
169 alteration of hydraulic heads due to water extraction and injection mainly depends on the aquifer's  
170 properties. A point-wise evaluation was therefore performed, based on available data on the hydrodynamic  
171 parameters of the unconfined aquifers. The maximum flow rate to be sustainably abstracted and injected  
172 was estimated and, from this value, the peak thermal power was derived. Differently from G.POT, the  
173 evaluation of open-loop geothermal potential did not consider a thermal load profile, but a peak value.  
174 Indeed, the evaluation of time-varying thermal loads would require complex and time-consuming  
175 numerical simulations for each point reported on the map, which is not feasible at this scale.  
176 The considerations reported above are the conceptual basis for the assessment and mapping of the  
177 geothermal potential for BHEs and GWHPs, which is described in this chapter.  
178



179

180

181

Fig. 4 – Maps of the hydrogeological parameters of the unconfined aquifers of Left Stura Bank and Right Stura Bank: (A) hydraulic heads and depth to water table; (B) transmissivity and saturated thickness. Scale 1:500,000.

182

### 183 3.1 Closed-loop geothermal potential

184

Closed-loop geothermal heat pumps can be installed virtually everywhere, since they do not require the abstraction of groundwater. However, the techno-economic feasibility of these systems varies substantially depending on a wide range of factors, namely:

187

- usage profile: the GSHP can be used in heating or cooling mode, or for both purposes in different proportions, depending on the building type (i.e. residential, commercial, public building...) and on the climate;

189

190

- thermal properties of the ground: thermal conductivity ( $\lambda$ ), thermal capacity ( $\rho c$ ), undisturbed ground temperature ( $T_0$ );

191

192

- BHE and plant properties: length ( $L$ ), minimum/maximum threshold fluid temperature ( $T_{lim}$ ) and thermal resistance ( $R_b$ ). The value of  $R_b$  is function of the geometry (borehole radius  $r_b$ , pipe

193

194 radius  $r_p$ , number of U-pipes  $n$ ) and of the thermal conductivity of the backfilling (geothermal grout  
 195  $\lambda_{bf}$ ).

196 Based on the aforementioned parameters, the closed-loop shallow geothermal potential  $\bar{P}_{BHE}$  (MWh/y)  
 197 was estimated with the G.POT method [27]:

$$\bar{P}_{BHE} = \frac{0.0701 \cdot (T_0 - T_{lim}) \cdot \lambda \cdot L \cdot t'_c}{G_{max}(u'_s, u'_c, t'_c) + 4\pi\lambda \cdot R_b}$$

198 Eq. 1

199 where  $T_0$  (°C) is the undisturbed ground temperature,  $T_{lim}$  (°C) is the threshold minimum fluid  
 200 temperature,  $\lambda$  (Wm<sup>-1</sup>K<sup>-1</sup>) is the ground thermal conductivity,  $L$  (m) is the borehole depth, and  $R_b$  (mKW<sup>-1</sup>)  
 201 is the borehole thermal resistance.  $G_{max}(u'_s, u'_c, t'_c)$  is function of three non-dimensional parameters  $t'_c$ ,  $u'_c$   
 202 and  $u'_s$ :

$$G_{max}(u'_s, u'_c, t'_c) = -0.619 \cdot t'_c \cdot \log(u'_s) + (0.532 \cdot t'_c - 0.962) \cdot \log(u'_c) - 0.455 \cdot t'_c - 1.619$$

203 Eq. 2

204 with:

$$t'_c = t_c / t_y$$

205 Eq. 3

$$u'_c = \rho c \cdot r_b^2 / (4\lambda t_c)$$

206 Eq. 4

$$u'_s = \rho c \cdot r_b^2 / (4\lambda t_s)$$

207 Eq. 5

208 where  $t_c$  (s) is the length of the heating season (set to 183 days), and  $t_y$  is the length of the year;  $\rho c$  (Jm<sup>-3</sup>K<sup>-1</sup>)  
 209 <sup>1</sup>) is the thermal capacity of the ground;  $t_s$  (s) is the simulated lifetime of the plant (set to 50 years). The  
 210 G.POT method is implemented in an electronic spreadsheet available at <http://goo.gl/Pm93JT>.

211 An only-heating usage profile was set, as most of residential buildings in Piedmont do not have a chilling  
 212 plant [35]. This is a conservative assumption, since the operation in cooling mode during summer would  
 213 partially compensate the heat extraction during winter, and hence reduce the thermal drift of the ground.  
 214 The thermal load has a sinusoidal trend and a typical duration of the heating season has been chosen, from  
 215 October 15<sup>th</sup> to April 15<sup>th</sup> (183 days), as foreseen by DPR 412/93 for the climate zone “E” [34]. A typical  
 216 double-U pipe BHE (Tab. 1) was considered, with a length  $L = 100m$ . The thermal properties of the ground  
 217 were therefore evaluated on the same depth.

218

219 **Tab. 1 – Geometrical and physical properties of the BHE adopted for the geothermal potential analysis.**

Parameter	Symbol	Value
Borehole length	$L$	100 m
Borehole radius	$r_b$	0.075 m

Pipe radius	$r_p$	0.016 m
Pipe number	$n$	4 (2-U pipe)
Thermal conductivity of backfilling	$\lambda_{bf}$	$2 \text{ Wm}^{-1}\text{K}^{-1}$

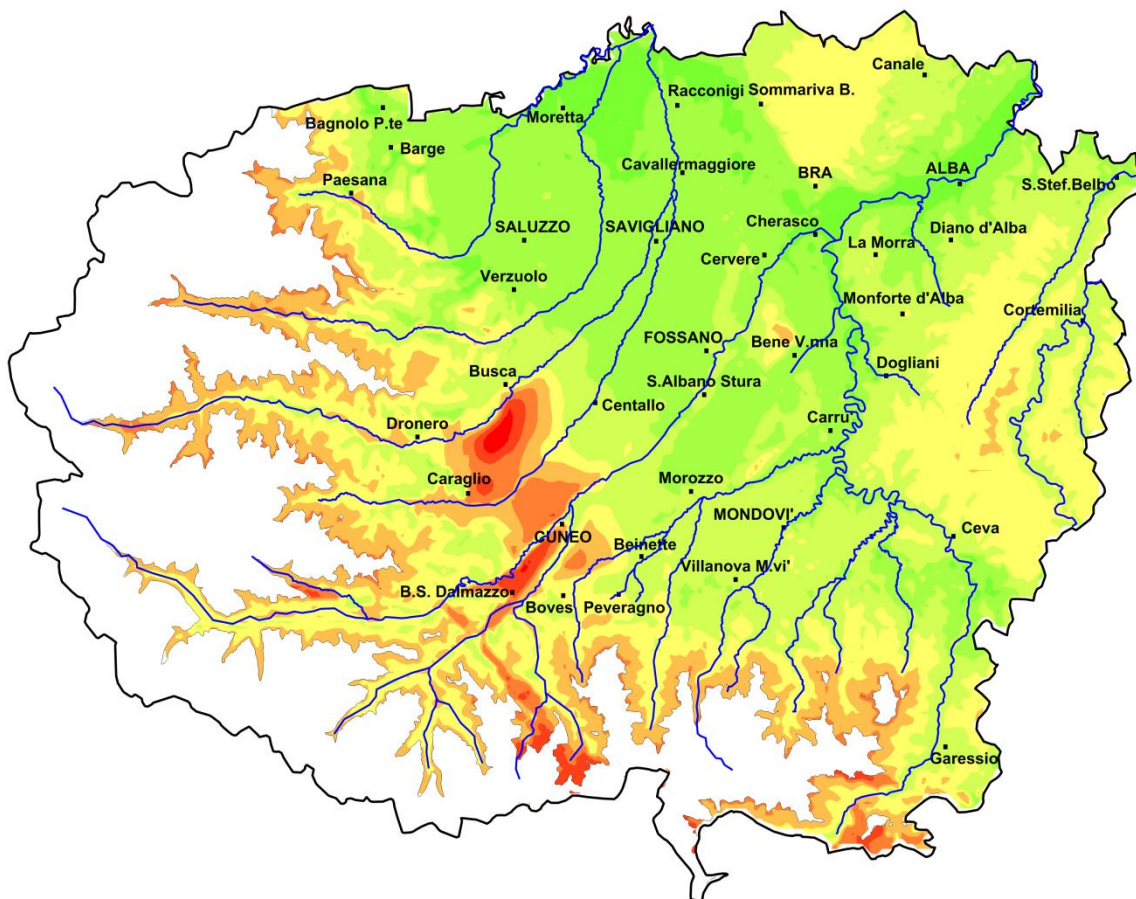
220

221 For thermal conductivity and thermal capacity, two different approaches were adopted:

222 - homogeneous values were adopted for compact rocks, both metamorphic (gneiss, serpentinite)  
 223 and sedimentary (marls, sandstones, limestones);

224 - a depth-averaged value has been chosen for alluvial aquifers in the plain, considering the different  
 225 thermal conductivity of the vadose and the saturated zone (see Tab. 2). The depth to water table  
 226 was used to determine the thickness of these two layers.

227 The maps of ground thermal conductivity and capacity are reported in the Supporting Information.



228

229 Fig. 5 – Map of the closed-loop geothermal potential calculated with the G.POT method [27]. Scale 1:750,000.

230

231

232

233 **Tab. 2 – Values of thermal conductivity and thermal capacity adopted for different lithologies (elaboration on data from [28, 45].**

N°	Lithology	$\lambda$ [ $Wm^{-1}K^{-1}$ ]	$\rho c$ [ $10^6 Jm^{-3}K^{-1}$ ]
1, 2	Alluvial/moraine sediments (dry)	2.4	1.5
1, 2	Alluvial/moraine sediments (saturated)	0.5	2.4
3, 9	Clay/Alternated clayey layers	1.8	2.5
4	Fine sand	1.8	2.5
5	Clay and clayey marl	2.1	2.25
6	Marl	2.3	2.25
7	Marl and siltstone	2.1	2.25
8	Sandstone	2.8	2.2
10	Serpentinite	2.5	2.8
11	Calceschyst	2.5	2.4
12	Limestone and dolostone	2.7	2.25
13	Fine grained gneiss	2.5	2.1
14	Coarse grained gneiss	2.9	2.1
15	Granite	3.2	2.5

234  
 235 The ground temperature is almost constant through the year and slightly higher than the annual mean air  
 236 temperature [30, 46], which is strongly correlated with the elevation (Fig. 2). A few data are available on  
 237 the subsurface temperature in the province of Cuneo, measured in a number of water wells in the plain  
 238 [31, 47], while no measures are available for the hilly and mountainous parts. An empirical correlation with  
 239 the ground elevation was therefore used, which was calibrated against ground temperature measured in  
 240 Switzerland [48]. The regional DTM of Piedmont was used as an input for ground elevations [49]. Ground  
 241 temperatures were not estimated above 1500 m a.s.l. where, according to Ref. [48], the correlation is not  
 242 valid since the snow cover alters the thermal exchange between the air and the ground. About 25% of the  
 243 total area of the province of Cuneo, but less than 1% of the total population, was therefore excluded from  
 244 the evaluation of the ground temperature and hence of the geothermal potential.

245 The map of the closed-loop geothermal potential is shown in Fig. 5 **Errore. L'origine riferimento non è stata**  
 246 **trovata..** This indicator varies from 5 to 12 MWh/y, depending on the thermal conductivity and the  
 247 temperature of the ground. In the central and northern part of the *Left Stura Bank* plain and in the *Tanaro*  
 248 *Valley*, the thermal conductivity is quite high ( $\lambda = 2 \div 2.3 Wm^{-1}K^{-1}$ ) due to the shallow water table, and  
 249 the ground temperature are the highest in the territory surveyed ( $T_0 = 12 \div 14^\circ C$ ). The highest  
 250 geothermal potentials ( $\bar{P}_{BHE} = 10 \div 12 MWh/y$ ) are therefore observed in this part of the plain, which  
 251 accounts for about 20% of the total area and 40% of the total population. The hills of Langhe and Roero and  
 252 the southern portion of the *Right Stura Bank* plain, which account for about 50% of the total population,  
 253 are slightly less suitable for BHEs ( $\bar{P}_{BHE} = 8 \div 10 MWh/y$ ) due to the lower thermal conductivity  
 254 ( $\lambda = 1.2 \div 2.1 Wm^{-1}K^{-1}$ ) and temperature ( $T_0 = 10 \div 12^\circ C$ ) of the ground. Less than 10% of the  
 255 population lives in areas with very low suitability for BHEs, where the geothermal potential falls to  
 256  $\bar{P}_{BHE} = 5 \div 8 MWh/y$ . The causes of such a low geothermal potential are different:

- 257 - in the valleys, the outcropping rocks are generally very conductive ( $\lambda > 2.5 \text{ Wm}^{-1}\text{K}^{-1}$ ) but the  
 258 ground temperature is very low ( $T_0 = 7 \div 10^\circ\text{C}$ );
- 259 - in the SW of the *Left Stura Bank* (Cuneo, Caraglio, Busca and Centallo) the water table is very deep  
 260 (up to 70 m from ground surface) and hence the thermal conductivity is very low ( $\lambda = 1 \div$   
 261  $1.5 \text{ Wm}^{-1}\text{K}^{-1}$ ). Borehole Thermal Energy Storage (BTES) can be installed here to take advantage  
 262 of the poorly conductive ground, storing large quantities of heat during Summer with low heat  
 263 losses [50].  
 264

### 265 3.2 Open-loop geothermal potential

266 While the design of closed-loop GSHPs is generally performed with standard sizing methods based on  
 267 ground thermal parameters which can be derived from large-scale geological maps, GWHPs require a  
 268 thorough hydrogeological characterization of the installation site. Indeed, the hydrodynamic properties of  
 269 the aquifer are site-specific, may vary in large ranges over short distances and should therefore be  
 270 evaluated with *in situ* tests. A spatially continuous map of the open-loop geothermal potential cannot be  
 271 developed unless a high spatial resolution database is available, which is not the case. A point-wise  
 272 evaluation was therefore performed. The maximum allowed flow rate was estimated for both extraction  
 273 and injection. The minimum of these two values was then used to calculate the open-loop geothermal  
 274 potential, i.e. the maximum thermal power that can be exchanged with the aquifer, if water is disposed  
 275 into the same aquifer after the heat exchange, which is the most commonly adopted practice.

276 Misstear and Beeson (2000, [51]) defined the potential well yield as the maximum flow rate that can be  
 277 extracted by a well respecting a low-level threshold called Deepest Advisable Pumping Water Level  
 278 (DAPWL). The variation of the hydraulic head in the well is calculated with the equation of Cooper and  
 279 Jacob (1946, [52]):

$$s_w(Q) = \frac{Q}{4\pi T} \cdot \log\left(2.25 \frac{T t_{pump}}{S r_w^2}\right) + CQ^2$$

280 Eq. 6

281 where  $Q$  ( $\text{m}^3\text{s}^{-1}$ ) is the well flow rate,  $T$  ( $\text{m}^2\text{s}^{-1}$ ) is the transmissivity of the aquifer,  $t_{pump}$  (s) is the pumping  
 282 time,  $r_w$  (m) is the well radius, and  $C$  ( $\text{s}^2\text{m}^{-5}$ ) is the coefficient of the quadratic term of the Rorabaugh  
 283 equation.

284 The drawdown in the production well and the rise in the reinjection well are calculated without considering  
 285 their mutual interference. This is a conservative assumption, since the drawdown induced by the extraction  
 286 well partially compensates the level rise due to the injection well, and vice versa.

287 The maximum allowed abstracted ( $Q_{abs}$ ) and injected ( $Q_{inj}$ ) flow rates were calculated with Eq. 6 imposing,  
 288 respectively, a maximum drawdown (Eq. 7) and a maximum level rise (Eq. 8).

$$s_w(Q_{abs}) = \alpha \cdot b$$

289

Eq. 7

$$s_w(Q_{inj}) = d - d_{min}$$

290

Eq. 8

291 where  $\alpha$  is a fraction of the saturated thickness ( $b$ ),  $d$  and  $d_{min}$  are respectively the initial and the  
 292 minimum possible depth of water table from ground surface. A 50% reduction of the initial saturated  
 293 thickness ( $\alpha = 0.5$ ), was set as suggested by Ref. [51], while a minimum water table depth  $d_{min} = 3m$  was  
 294 imposed to provide a safety margin against groundwater flooding.

295 The values of transmissivity ( $T$ ) were drawn from a dataset of specific flow rates  $q_{sp}$  derived from 304 wells  
 296 in the *Left and Right Stura Bank* [53], adopting the equivalence  $T = q_{sp}$  suggested by Refs. [54-56]. The  
 297 storage coefficient was set to  $S = 0.2$ , i.e. the average value of the range ( $S = 0.1 \div 0.3$ ) provided for  
 298 unconfined aquifers [54]. The well radius was set to  $r_w = 0.25m$  and the quadratic loss coefficient of the  
 299 Rorabaugh equation was set to  $C = 1900s^2m^{-5}$ , i.e. the highest value for a non-deteriorated well [57].  
 300 The pumping time was set to  $t_{pump} = 200d$ , as suggested by Ref. [51].

301 The maximum allowed extracted/injected flow rates are used as input to calculate the open-loop  
 302 geothermal potential according to two operating modes:

303 - without reinjection, thus avoiding possible groundwater flooding issues in the reinjection wells:

$$P_{GWHP,max,noinj} = Q_{abs} \cdot \rho_f c_f \cdot \Delta T$$

304

Eq. 9

305 - with reinjection, which is the most commonly adopted solution:

$$P_{GWHP,max,inj} = \min(Q_{abs}, Q_{inj}) \cdot \rho_f c_f \cdot \Delta T$$

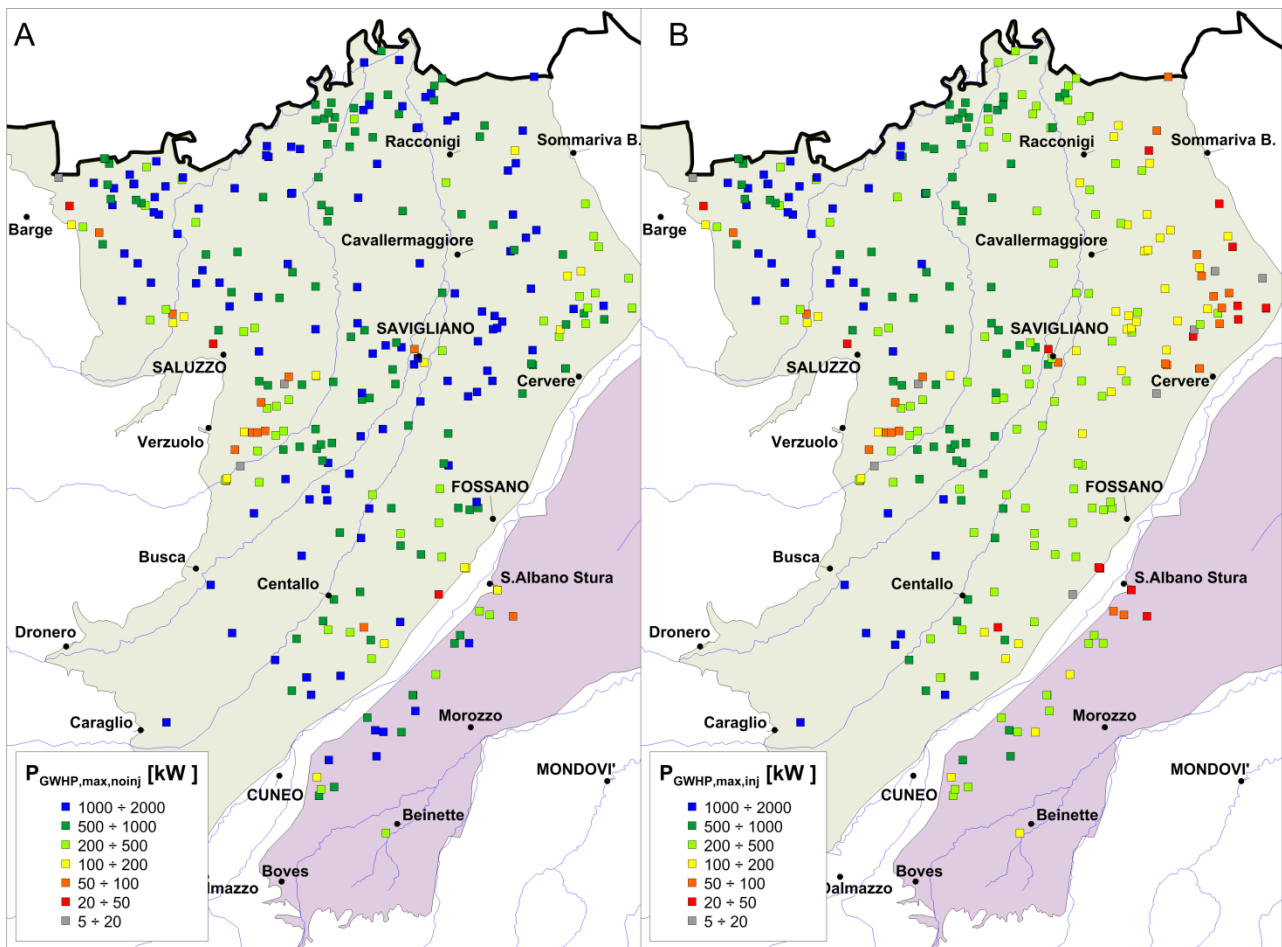
306

Eq. 10

307 where  $\rho_f c_f = 4.2 \cdot 10^6 Jm^{-3}K^{-1}$  is the thermal capacity of water and  $\Delta T = 5K$  is the temperature  
 308 difference between injection and abstraction well.

309 The maps of the open-loop geothermal potential with and without reinjection are reported in Fig. 6.  
 310 Reinjection can be avoided if a surface water body (rivers, channels, lakes) is available close to the  
 311 installation site. The open-loop geothermal potential in this case achieves values higher than 1000 kW in  
 312 most of the *Left Stura Bank* plain, as shown in Fig. 6A, while lower values are observed on the western and  
 313 eastern edges, due to the lower transmissivity of the aquifer (Fig. 4B). However, reinjection is usually  
 314 required for GWHPs in Piedmont, in order to avoid additional consumptive uses of the aquifer, and hence  
 315 the open-loop geothermal potential with reinjection was calculated ( $P_{GWHP,max,inj}$ , see Eq. 10). Reinjection  
 316 proves a strong limiting factor for the installable thermal power of GWHPs, as shown in Fig. 6B, due to the  
 317 low depth to water table of the northern and eastern sectors of the *Left Stura Bank*, and of most of the  
 318 *Right Stura Bank* (Fig. 4A). A clear decreasing trend from west to east is therefore observed for open-loop

319 geothermal potential in the *Left Stura Bank* (Fig. 4B) due to the progressive reduction of the water table  
 320 depth and hence of the injectable flow rate. This issue can be overcome adopting multiple injection and  
 321 extraction wells, or other reinjection techniques such as ponds or trenches [58].  
 322 Groundwater chemistry is another important design issue for of GWHPs. According to Rafferty (1999, [59]),  
 323 scale formation can occur in the thermal exchange circuit for water carbonate hardness higher than 10°F.  
 324 This threshold is usually not respected in the unconfined aquifer in the province of Cuneo, with most values  
 325 ranging between 20°F and 40°F [38, 60], and hence the use of secondary heat exchange circuit is strongly  
 326 advised.  
 327



328  
 329 **Fig. 6 – Map of the open-loop geothermal potential in the alluvial shallow aquifers of the province of Cuneo with water disposal**  
 330 **in surface water bodies (A) and in the same aquifer (B).**

### 331 4 Conclusions

332 Ground Source Heat Pump is an environmentally and economically viable technology for the heating and  
 333 cooling of buildings. It exploits a local RES such as the heat stored in shallow ground. This resource is  
 334 available everywhere, but the techno-economic feasibility depends on the site conditions, i.e. ground  
 335 thermal and/or hydrogeological parameters. In this work, the potential for the installation of closed-loop

336 and open-loop geothermal heat pumps was assessed in the province of Cuneo, NW Italy. The geology, the  
337 hydrogeology and the climate of this territory was studied by harmonizing and homogenizing data from  
338 different sources. Based on these data, relevant parameters for the operation of GSHPs were estimated. A  
339 mathematical method called G.POT [27] was used to estimate the closed-loop geothermal potential, i.e. the  
340 thermal power that can be exchanged by a BHE. The open-loop geothermal potential is defined as the  
341 maximum thermal power that can be exchanged by a GWHP composed of a well doublet. The thermal  
342 power is limited by hydraulic head alterations induced by groundwater extraction and injection, which  
343 depend on the hydrogeological properties of the aquifer.

344 According to the results, the following conclusions can be drawn:

- 345 - the province of Cuneo has a good potential for the installation of closed-loop BHEs, in particular in  
346 the central part of the plain, where about 40% of the population lives. In this area, 10÷12 MWh/y  
347 can be exchanged with a 100 m-long BHE. The geothermal potential diminishes to 8÷10 MWh/y in  
348 the hilly areas of the Langhe and Roero, in the alluvial aquifers at the bottom of the valleys and in  
349 the southern part of the alluvial plain of the *Right Stura Bank*, due to lower ground temperatures;
- 350 - less than 10% of the population lives in areas with a low suitability for the installation of BHEs,  
351 where the geothermal potential falls to  $\bar{P}_{BHE} = 5 \div 8 \text{ MWh/y}$ . In the south-western part of the  
352 plain (both *Left Stura Bank* and *Right Stura Bank*), this is due to the presence of a thick vadose zone  
353 (up to 70 m) and the consequently low thermal conductivity of the ground. On the other hand, such  
354 a thick unsaturated zone makes this area suitable for Borehole Thermal Energy Storage (BTES). The  
355 upper part of the Alpine valleys, characterized by a very low ground temperature, is also scarcely  
356 suitable for BHEs;
- 357 - a large part of the Province of Cuneo is occupied by alluvial aquifers with a high transmissivity,  
358 which makes them suitable for the installation of GWHPs. The main limiting factor is the low depth  
359 to water table, which is critical for water reinjection. This issue can be overcome by using  
360 reinjection techniques such as ponds, trenches, and gabions [58].

361 Maps of geothermal potential are valuable tools for the evaluation of the suitability for closed-loop and  
362 open-loop geothermal heat pumps. Closed-loop BHEs can be installed everywhere, hence the evaluation in  
363 this work focused on the efficiency of a possible installation, depending on site-specific ground thermal  
364 parameters. On the other hand, the installation of an open-loop GWHP is possible only in the presence of a  
365 sufficiently productive aquifer. For this reason, the evaluation focused on the sustainability of groundwater  
366 extraction and reinjection, which depends on the hydrodynamic properties of the aquifer, while the  
367 efficiency was not evaluated, since it depends on the characteristics of single geothermal systems.

## 368 Acknowledgements

369 Financial support for this work was provided by Fondazione Cassa di Risparmio di Cuneo in the framework  
370 of the project “Survey and mapping of the potentiality of Geothermal Heat Pumps in the Province of  
371 Cuneo”.

## 372 5 References

- 373 [1] European Commission, Europe 2020 targets.  
374 <[http://ec.europa.eu/eurostat/documents/4411192/4411431/Europe\\_2020\\_Targets.pdf](http://ec.europa.eu/eurostat/documents/4411192/4411431/Europe_2020_Targets.pdf)>, 2015 (accessed  
375 December 21st, 2015.).
- 376 [2] Gestore Servizi Energetici, Rapporto Statistico energia da fonti rinnovabili anno 2013 [2013 statistical  
377 report on renewable energy], GSE, 2015.
- 378 [3] European Commission, Energy roadmap 2050, 2012.
- 379 [4] H. Herich, M.F.D. Gianini, C. Piot, G. Močnik, J.L. Jaffrezo, J.L. Besombes, A.S.H. Prévôt, C. Hueglin,  
380 Overview of the impact of wood burning emissions on carbonaceous aerosols and PM in large parts of the  
381 Alpine region, Atmospheric Environment 89 (2014) 64-75.
- 382 [5] M.C. Pietrogrande, D. Bacco, S. Ferrari, J. Kaipainen, I. Ricciardelli, M.L. Riekkola, A. Trentini, M. Visentin,  
383 Characterization of atmospheric aerosols in the Po valley during the supersito campaigns - Part 3:  
384 Contribution of wood combustion to wintertime atmospheric aerosols in Emilia Romagna region (Northern  
385 Italy), Atmospheric Environment 122 (2015) 291-305.
- 386 [6] P. Blum, G. Campillo, W. Münch, T. Kölbel, CO2 savings of ground source heat pump systems – A  
387 regional analysis, Renewable Energy 35(1) (2010) 122-127.
- 388 [7] D. Saner, R. Juraske, M. Kübert, P. Blum, S. Hellweg, P. Bayer, Is it only CO2 that matters? A life cycle  
389 perspective on shallow geothermal systems, Renewable and Sustainable Energy Reviews 14(7) (2010) 1798-  
390 1813.
- 391 [8] ISPRA, Fattori di emissione atmosferica di CO2 e sviluppo delle fonti rinnovabili nel settore idroelettrico,  
392 in: ISPRA (Ed.) ISPRA, Roma, Italy, 2015, p. 75.
- 393 [9] G. Florides, S. Kalogirou, Ground heat exchangers—A review of systems, models and applications,  
394 Renewable Energy 32(15) (2007) 2461-2478.
- 395 [10] M. Antics, R. Bertani, B. Sanner, Summary of EGC 2013 Country Update Reports on Geothermal Energy  
396 in Europe, European Geothermal Conference, Pisa (Italy), 2013, pp. 1-18.
- 397 [11] Unione Geotermica Italiana, Growth forecast of geothermal energy in Italy by 2030 - for a new Italian  
398 geothermal manifesto, UGI, 2011.
- 399 [12] Eurostat, Half-yearly electricity and gas prices 2014 - Semester 2, 2015.
- 400 [13] ENEA, Rapporto annuale efficienza energetica 2015, 2015.
- 401 [14] A. Casasso, R. Sethi, Tecnologia e potenzialità dei sistemi geotermici a bassa entalpia, Geingegneria  
402 Ambientale e Mineraria 138(1) (2013) 13-22.
- 403 [15] F. Rizzi, M. Frey, F. Iraldo, Towards an integrated design of voluntary approaches and standardization  
404 processes: An analysis of issues and trends in the Italian regulation on ground coupled heat pumps, Energy  
405 Conversion and Management 52(10) (2011) 3120-3131.
- 406 [16] UNI, UNI 11466:2012 Sistemi geotermici a pompa di calore - Requisiti per il dimensionamento e la  
407 progettazione [Heat pump geothermal systems - Design and sizing requirements], 2012.
- 408 [17] UNI, UNI 11467:2012 Sistemi geotermici a pompa di calore - Requisiti per l'installazione [Heat pump  
409 geothermal systems - Installation requirements], 2012.
- 410 [18] UNI, UNI 11468:2012 Sistemi geotermici a pompa di calore - Requisiti ambientali [Heat pump  
411 geothermal systems - Environmental requirements], 2012.

412 [19] B.M.S. Giambastiani, F. Tinti, D. Mendrinis, M. Mastrocicco, Energy performance strategies for the  
413 large scale introduction of geothermal energy in residential and industrial buildings: The GEO.POWER  
414 project, *Energy Policy* 65(0) (2014) 315-322.

415 [20] F. Tinti, A. Pangallo, M. Berneschi, D. Tosoni, D. Rajver, S. Pestotnik, D. Jovanović, T. Rudinica, S. Jelisić,  
416 B. Zlokapa, A. Raimondi, F. Tollari, A. Zamagni, C. Chiavetta, J. Collins, M. Chieco, A. Mercurio, F. Marcellini,  
417 D. Mrvaljević, M. Meggiolaro, How to boost shallow geothermal energy exploitation in the adriatic area: the  
418 LEGEND project experience, *Energy Policy* 92 (2016) 190-204.

419 [21] V. Somogyi, V. Sebestyén, G. Nagy, Scientific achievements and regulation of shallow geothermal  
420 systems in six European countries – A review, *Renewable and Sustainable Energy Reviews*.

421 [22] A. Casasso, R. Sethi, Efficiency of closed loop geothermal heat pumps: A sensitivity analysis, *Renewable*  
422 *Energy* 62 (2014) 737-746.

423 [23] A. Casasso, R. Sethi, Sensitivity Analysis on the Performance of a Ground Source Heat Pump Equipped  
424 with a Double U-pipe Borehole Heat Exchanger, *Energy Procedia* 59(0) (2014) 301-308.

425 [24] A. Casasso, R. Sethi, Modelling thermal recycling occurring in groundwater heat pumps (GWHPs),  
426 *Renewable Energy* 77(0) (2015) 86-93.

427 [25] T. Arola, L. Eskola, J. Hellen, K. Korkka-Niemi, Mapping the low enthalpy geothermal potential of  
428 shallow Quaternary aquifers in Finland, *Geothermal Energy* 2(1) (2014) 9.

429 [26] S. Busoni, A. Galgaro, E. Destro, Geoscambio nella Provincia di Treviso, Provincia di Treviso - Servizio  
430 Ecologia e Ambiente, 2012.

431 [27] A. Casasso, R. Sethi, G.POT: A quantitative method for the assessment and mapping of the shallow  
432 geothermal potential, *Energy* 106 (2016) 765-773.

433 [28] E. Di Sipio, A. Galgaro, E. Destro, G. Teza, S. Chiesa, A. Giaretta, A. Manzella, Subsurface thermal  
434 conductivity assessment in Calabria (southern Italy): a regional case study, *Environmental Earth Sciences*  
435 (2014) 1-19.

436 [29] A. Galgaro, E. Di Sipio, G. Teza, E. Destro, M. De Carli, S. Chiesa, A. Zarrella, G. Emmi, A. Manzella,  
437 Empirical modeling of maps of geo-exchange potential for shallow geothermal energy at regional scale,  
438 *Geothermics* 57 (2015) 173-184.

439 [30] A. Gemelli, A. Mancini, S. Longhi, GIS-based energy-economic model of low temperature geothermal  
440 resources: A case study in the Italian Marche region, *Renewable Energy* 36(9) (2011) 2474-2483.

441 [31] S. Lo Russo, M. Civita, Hydrogeological and thermal characterization of shallow aquifers in the plain  
442 sector of Piemonte region (NW Italy): implications for groundwater heat pumps diffusion, *Environmental*  
443 *Earth Sciences* 60(4) (2010) 703-713.

444 [32] Regione Piemonte, Piano di Tutela delle Acque della Regione Piemonte, Regione Piemonte, 2007.

445 [33] ARPA Piemonte, Regione Piemonte, Banca dati idrologica e di qualità acque superficiali [Data bank of  
446 hydrology and surface water quality], in: ARPA Piemonte (Ed.) Torino, 2015.

447 [34] Repubblica Italiana, DPR 412/1993 - Regolamento recante norme per la progettazione, l'installazione,  
448 l'esercizio e la manutenzione degli impianti termici degli edifici ai fini del contenimento dei consumi di  
449 energia, in attuazione dell'art. 4, comma 4, della legge 9 gennaio 1991, n. 10., 1993.

450 [35] ISTAT, I consumi energetici delle famiglie [Energy consumption of Italian families], ISTAT, Roma, 2014.

451 [36] O.A. Pfiffner, *Geology of the Alps*, 2nd edition ed., John Wiley & Sons, Chichester, UK, 2014.

452 [37] ARPA Piemonte, Carta geologica del Piemonte, scala 1:250000., in: ARPA Piemonte (Ed.) ARPA  
453 Piemonte, 2012.

454 [38] M.V. Civita, B. Vigna, M. De Maio, A. Fiorucci, S. Pizzo, M. Gandolfo, C. Banzato, S. Menegatti, M. Offi,  
455 B. Moitre, *Le acque sotterranee della pianura e della collina cuneese*, Scribo2011.

456 [39] P. Faletti, R. Gelati, S. Rogledi, Oligo-Miocene evolution of Monferrato and Langhe, related to deep  
457 structures, in: R. Polino, R. Sacchi (Eds.), *Rapporti Alpi-Appennino*, Accademia Nazionale delle Scienze,  
458 Rome, 1995, pp. 1-19.

459 [40] ARPA Piemonte, Geological map of Piemonte Region, scale 1:100000, in: ARPA Piemonte (Ed.) ARPA  
460 Piemonte.

461 [41] S. Lo Russo, L. Gnani, E. Rocca, G. Taddia, V. Verda, Groundwater Heat Pump (GWHP) system modeling  
462 and Thermal Affected Zone (TAZ) prediction reliability: Influence of temporal variations in flow discharge  
463 and injection temperature, *Geothermics* 51 (2014) 103-112.

464 [42] E. Milnes, P. Perrochet, Assessing the impact of thermal feedback and recycling in open-loop  
465 groundwater heat pump (GWHP) systems: a complementary design tool, *Hydrogeol J* 21(2) (2013) 505-514.

466 [43] V.A. Fry, Lessons from London: Regulation of open-loop ground source heat pumps in central London,  
467 *Quarterly Journal of Engineering Geology and Hydrogeology* 42(3) (2009) 325-334.

468 [44] A. García-Gil, E. Vázquez-Suñe, M.M. Alcaraz, A.S. Juan, J.Á. Sánchez-Navarro, M. Montlleó, G.  
469 Rodríguez, J. Lao, GIS-supported mapping of low-temperature geothermal potential taking groundwater  
470 flow into account, *Renewable Energy* 77(0) (2015) 268-278.

471 [45] VDI, VDI 4640 - Thermal use of underground, Blatt 1: Fundamentals, approvals, environmental aspects,  
472 2010.

473 [46] M. Ouzzane, P. Eslami-Nejad, M. Badache, Z. Aidoun, New correlations for the prediction of the  
474 undisturbed ground temperature, *Geothermics* 53(0) (2015) 379-384.

475 [47] ARPA Piemonte, Indagine geotermometrica sui piezometri della rete di monitoraggio quantitativa  
476 regionale [Geo-thermometric survey on the piezometers of the regional quantitative groundwater  
477 monitoring network], 2009, pp. 1-35.

478 [48] S. Signorelli, T. Kohl, Regional ground surface temperature mapping from meteorological data, *Global  
479 and Planetary Change* 40(3-4) (2004) 267-284.

480 [49] Regione Piemonte, Digital Terrain Model with 10 meters resolution.  
481 <[http://www.dati.piemonte.it/catalogodati/dato/100291-modelli-digitali-del-terreno-da-ctrn-1-10000-  
482 passo-10mt-modello-altezze-filtrato.html](http://www.dati.piemonte.it/catalogodati/dato/100291-modelli-digitali-del-terreno-da-ctrn-1-10000-passo-10mt-modello-altezze-filtrato.html)>, 2000 (accessed January 8th, 2015.).

483 [50] N. Giordano, C. Comina, G. Mandrone, A. Cagni, Borehole thermal energy storage (BTES). First results  
484 from the injection phase of a living lab in Torino (NW Italy), *Renewable Energy* 86 (2016) 993-1008.

485 [51] B.D.R. Misstear, S. Beeson, Using operational data to estimate the reliable yields of water-supply wells,  
486 *Hydrogeol J* 8(2) (2000) 177-187.

487 [52] C.E. Jacob, Effective radius of drawdown test to determine artesian well, *Proceeding of the American  
488 Society of Civil Engineers, ASCE*, 1946, pp. 629-646.

489 [53] Regione Piemonte, Dati di portata specifica ricavati da prove di pompaggio e stratigrafie di pozzi  
490 superficiali - PTA: Monografie di area idrogeologica. - UTM WGS84 [Specific flow rate from pumping tests  
491 and shallow well stratigraphies - Water Protection Plan: hydrogeological area monograph], in: R. Piemonte  
492 (Ed.) 2003.

493 [54] A. Di Molfetta, R. Sethi, *Ingegneria degli Acquiferi*, Springer 2012.

494 [55] F.G. Driscoll, *Groundwater and wells*, 2nd ed., St. Paul, Minnesota, 1986.

495 [56] B. Misstear, D. Banks, L. Clark, *Water wells and boreholes*, 2006.

496 [57] W.C. Walton, *Selected analytical methods for well and aquifer evaluation*, Illinois State Water Survey,  
497 1962.

498 [58] H. Bouwer, Artificial recharge of groundwater: hydrogeology and engineering, *Hydrogeol J* 10(1) (2002)  
499 121-142.

500 [59] K. Rafferty, Well pumping issues in commercial groundwater heat pump systems, in: Anon (Ed.)  
501 *Geothermal Resources Council, Burlingame, CA, USA*, 1997, pp. 81-85.

502 [60] G. Ansaldo, B. Maffeo, *Inventario delle risorse idriche della Provincia di Cuneo - Parte VI - Le acque  
503 sotterranee della pianura cuneese (alla sinistra della Stura di Demonte)*, in: P.d. Cuneo (Ed.) 1981, p. 117.  
504  
505  
506

507 **6 List of acronyms**

ASHP	Air-Source Heat Pump	508
BHE	Borehole Heat Exchangers	
BP	Before Present	509
BTES	Borehole Thermal Energy Storage	
COP	Coefficient Of Performance	
DD	Degree-Days	
DTM	Digital Terrain Model	
EU	European Union	
G.POT	Geothermal POTential	
GSHP	Ground Source Heat Pump	
GWHP	Ground Water Heat Pump	
RES	Renewable Energy Source	

510

511

512 **7 List of symbols**

513 **7.1 Latin letters**

Symbol	Unit	Description
$b$	m	Saturated thickness of the aquifer
$d$	m	Depth of the aquifer's water table (depth to water table)
$d_{min}$	m	Minimum allowed depth to water table
$G_{max}(u'_s, u'_c, t'_c)$	-	Non-dimensional function of the maximum thermal alteration of the ground at the borehole wall
$L$	m	Depth of the borehole heat exchanger
$n$	-	Number of pipes
$\bar{P}_{BHE}$	MWh/y	Closed-loop geothermal potential
$P_{GWHP,max,inj}$	kW	Open-loop geothermal potential with water reinjection into the same aquifer
$P_{GWHP,max,noinj}$	kW	Open-loop geothermal potential without water reinjection
$Q$	$m^3s^{-1}$	Well flow rate
$Q_{abs}$	$m^3s^{-1}$	Maximum allowed abstraction flow rate
$Q_{inj}$	$m^3s^{-1}$	Maximum allowed injection flow rate
$q_{sp}$	$m^2s^{-1}$	Specific flow rate
$r_b$	m	Radius of the borehole
$R_b$	$mKW^{-1}$	Borehole thermal resistance
$r_p$	m	Radius of the pipes of the borehole heat exchanger
$r_w$	m	Well radius
$S$	-	Aquifer's storage coefficient
$s_w$	m	Level displacement in the well
$T_0$	K	Undisturbed ground temperature
$t_c$	s	Length of the heating season
$t'_c$	-	Non-dimensional length of the heating season
$T$	$m^2s^{-1}$	Aquifer's transmissivity
$T_{lim}$	K	Minimum or maximum threshold temperature of the heat carrier fluid
$T_{mth}$	°C	Monthly average air temperature
$t_s$	s	Simulated operation time
$t_y$	s	Length of the year
$T_{yr}$	°C	Yearly average air temperature
$u'_c$	-	Non-dimensional cycle time parameter
$u'_s$	-	Non-dimensional simulation time parameter

514 **7.2 Greek letters**

Symbol	Unit	Description
$\alpha$	-	Maximum allowed reduction of the saturated thickness
$\Delta T$	K	Temperature difference between abstraction and injection well
$\lambda$	$Wm^{-1}K^{-1}$	Thermal conductivity of the ground
$\lambda_{bf}$	$Wm^{-1}K^{-1}$	Thermal conductivity of the borehole filling (grout)
$\rho c$	$Jm^{-3}K^{-1}$	Thermal capacity of the ground
$\rho_f c_f$	$Jm^{-3}K^{-1}$	Thermal capacity of water

515